Bulgarian Journal of Physics vol. **51** (2024) 411–420

Re-Examination of Tidal Wave Behaviour in Mass $98 \leq A \leq 118$

A. Choudhary[1], **V. Kumar**[1], **A. Shukla**[1], **Y. P. Singh**[1], **T. Tripathi**[1], **Virendra Kumar**[1], **P. Jain**[2], **O. P. Chauhan**[2], **Y. Kumar**[3], **S. Kumar**[3]

[1]Physics Department, University of Lucknow, Lucknow, 226007 India
[2]Department of Physics, Sri Aurobindo College, University of Delhi, 110017, India
[3]Department of Physics, Hansraj College, University of Delhi, 110007 India
*Corresponding author E-mail: vinod2.k2@gmail.com

Received: 28 November 2024
doi: https://doi.org/10.55318/bgjp.2024.51.4.411

Abstract. Studies of nuclear structure in the mass range $98 \leq A \leq 118$ reveal diverse collective phenomena, including rotational, vibrational, and transitional behaviors. Recent investigations have highlighted the potential for tidal wave behavior—a unique form of nuclear excitation. This phenomenon characterized by distinct experimental fingerprints, merits a detailed re-examination to advance our understanding of its underlying mechanisms.

KEY WORDS: Nuclear Structure, Collective Band, Reduced Transition Probability, Tidal Wave.

1 Introduction

The deformed nuclei showed almost constant $B(E2)$ values with spin and followed the characteristics of rotational energy $E_x = \frac{\hbar^2}{2\Im} I(I+1)$. Nuclei near magic numbers show vibrational characteristics, where the energy of the states follows $E = n\hbar\omega$, and $B(E2)$ values increase with spin, with $B(E2) \propto n \propto I$. It is noticed that in most cases, the mid-shell region shows deformed characteristics. As one moves toward magic numbers (spherical), the nuclei tend toward vibrational characteristics. The region where the energy of states follows rotational characteristics and $B(E2)$ starts increasing with spin is analogous to the rotation of the nuclear mean field causing vibrations in nuclei, similar to how the Moon's rotation causes tidal waves in the sea. This phenomenon is referred to as a 'tidal wave' in nuclei [1, 2]. On the other hand, when $B(E2)$ increases with spin and the energy of states follows vibrational characteristics, such a band is called a vibrational band.

The lowest-energy state, at a given angular momentum, is called a yrast state, and such states hold a special status in nuclear structure physics. Low-energy nuclear excitations are generally understood as being due either to individual nucleon (intrinsic) motions or to collective rotations and vibrations. The key difference between the vibrator and rotor is that the angular momentum of an ideal rotor is generated by increasing angular velocity, whereas, in the ideal vibrator, angular velocity remains constant (equal to half the vibrational frequency) and angular momentum is generated by increasing the wave amplitude. In general, nuclei lie between these idealized limits; i.e., both deformation and angular velocity increase with angular momentum.

The structures built upon the $K^\pi = 43/2^{(-)}$ and $K^\pi = 43/2^{(+)}$ isomers in ^{183}Os [3] and the $K^\pi = 25^+$ isomer in ^{182}Os [1] are irregular and appear to form vibrational-like sequences. These structures contrast with the behaviour of strongly coupled collective rotational bands, which are usually associated with high-K isomers. Note how the γ-ray energies are almost constant as the spin increases in the sequences above the $K^\pi = 43/2^{(-)}$, $K^\pi = 43/2^{(+)}$ and $K^\pi = 25^+$ isomers, see Figure 1. A sequence of collective transitions would be expected to have gradually increasing transition energies, proportional to spin. The structure consists of two irregular sequences of interlinked $E2$ transitions (see Figure 1), with one sequence being more strongly populated than the other. In a normal rotational band, angular momentum gain results from increasing

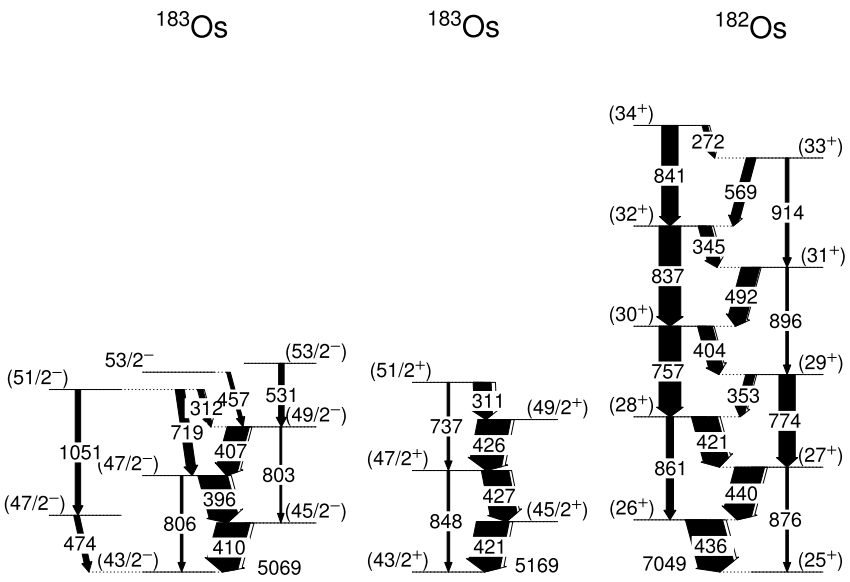

Figure 1. Partial Level scheme deduced for the transitions above $K^\pi = 43/2^{(-)}$, $K^\pi = 43/2^{(+)}$ and $K^\pi = 25^+$ isomeric states in ^{182,183}Os [1,3].

angular frequency at an approximately constant shape. Thus, in this interpretation, the collective structure based on the $K^\pi = 43/2^{(-)}$, $K^\pi = 43/2^{(+)}$ and $K^\pi = 25^+$ isomers in ^{183}Os [3], ^{182}Os [1], is very different from a normal rotational band. Instead, it resembles a multiphonon band or the so-called nuclear tidal wave.

The present work focuses on re-examining the tidal wave behavior in mass $A \sim 100$, based on the theoretical calculations by Frauendorf et al. [2] using the shell-correction version of the Tilted Axis Cranking model. For weakly or slightly deformed nuclei, the predictions required two experimental fingerprints to be observed simultaneously: the energy sequence of the levels followed rotational characteristics, and the $B(E2)$ values increased with spin. Generally, rotational bands are observed in deformed nuclei, with $B(E2)$ values remaining almost constant with spin. For vibrational bands, $B(E2)$ values increase with spin; however, the energy sequence of the levels does not follow rotational characteristics. Another fingerprint is that the angular momentum (I) increases as the amplitude of the wave increases, while the angular velocity (ω) remains constant. The vibrational band of tidal waves would appear as a vertical line in an $I(\omega)$ plot.

2 Systematics of Tidal Wave Fingerprints

2.1 Plots of I (ω) and derived slope $\rho = \triangle I/\triangle\omega$

In the case of rotor-like behavior, the angular momentum $I = \Im\omega$ increases linearly with the angular velocity ω, while the moment of inertia $\Im$ remains constant. The rotational energy is expressed as $E_{\text{rot}} = \frac{1}{2}\Im\omega^2 = I^2/(2\Im)$, and it is quadratic in both ω or I. In the case of vibrator-like behavior, both E and I increase due to an increase in $\Im$ (or equivalently, an increase in the radius r). The deformation strongly increases with I, while ω remains nearly constant. For rotor-like nuclei, the deformation remains nearly constant, while $I \propto \omega$. The transition between vibrational and rotational regimes occurs gradually.

The vibrational band of tidal waves would appear as a vertical line in an $I(\omega)$ plot. As a rule, vibrations in real nuclei are substantially anharmonic. In $I(\omega)$ plots, anharmonic tidal waves will have a finite slope ($\rho = \triangle I/\triangle\omega$) and intercept the ω axis. However, real nuclei lie between these idealized limits; i.e., both deformation and angular velocity increase with angular momentum. Figure 2 shows the values of ρ in the $I(\omega)$ plots for nuclei with masses $98 \leq A \leq 118$. Nuclei with the maximum values of ρ may exhibit tidal nature at low-spin states. The ratio $R_{4^+/2^+}$ and the ρ values for selected nuclei are listed in Table 1. We speculate that the nuclei ^{108,110}Pd and ^{104,110}Cd may exhibit evidence of tidal wave behavior based on their $I(\omega)$ plots.

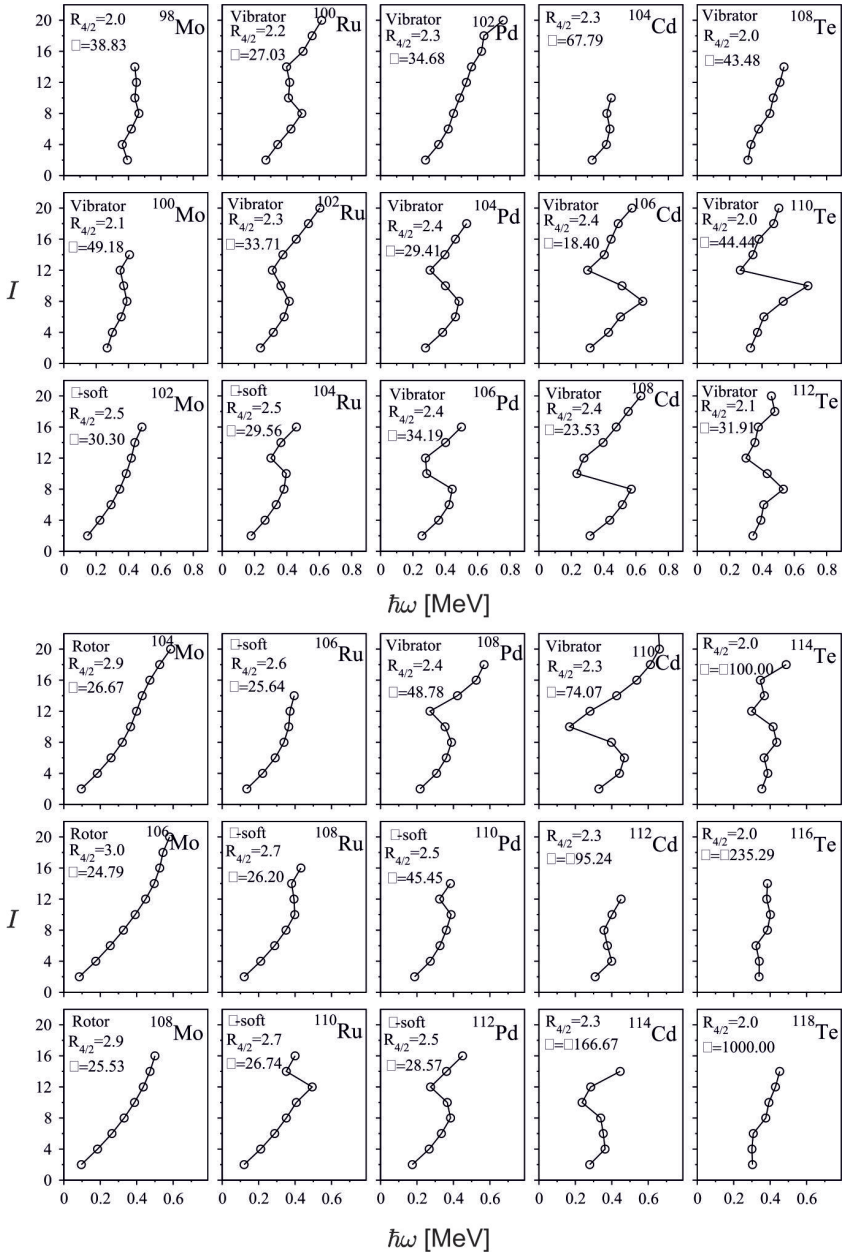

Figure 2. $I(\omega)$ plots and data from Refs. [6–26]. The values of $\rho = \triangle I/\triangle\omega$ was calculated for the points seems to be in a straight line by least square fit method. See text for details

Table 1. Listed values are for the $\rho = \triangle I/\triangle\omega$ and $\alpha = \triangle B(E2)/\triangle I$

Isotopes	$\rho = \frac{\triangle I}{\triangle\omega}$	$\alpha = \frac{\triangle B(E2)}{\triangle I}$	Isotopes	$\rho = \frac{\triangle I}{\triangle\omega}$	$\alpha = \frac{\triangle B(E2)}{\triangle I}$
^{100}Mo	49.18		^{104}Cd	67.79	
^{106}Pd	34.19	0.029	^{110}Cd	74.07	0.025
^{108}Pd	48.78	0.050	^{114}Cd	-166.67	0.072
^{110}Pd	45.45	0.040	^{108}Te	43.48	
^{104}Ru	29.56	0.038	^{110}Te	44.44	
			^{118}Te	1000	

2.2 Reduced transition probability $B(E2)$ versus the nuclear spin I

In nuclear structure textbooks [27, 28], two types of collective excitations are distinguished: rotations and vibrations. The $B(E2)$ values reflect nuclear deformation. The $B(E2)$ values for a perfect rotor are described in detail in [27, 28].

$$B(E2) = \frac{5}{16\pi} Q_0^2 \langle I_i K 20 \mid I_f K\rangle^2 \ \ [\mathrm{e}^2\mathrm{fm}^4]\,,$$
$$Q_0 = \sqrt{\frac{16\pi}{5}}\frac{3}{4\pi} ZeR^2\beta\,,$$

where β is the quadrupole deformation parameter [29].

$$B(E2) \propto \frac{3I(I-1)(I+1)}{(2I-2)(2I-1)(2I+1)} \sim \frac{3}{8}\,.$$

Rotation corresponds to a fixed deformed surface, where the reduced transition probability $B(E2)$ values remain nearly constant with increasing angular momentum I.

Yrast vibrational nuclei consist of a sequence of stacked d-boson, which align their angular momenta. In the ideal case of n non-interacting bosons, the reduced transition probability $B(E2)$ from n phonon state ($2n = I$) is define as in Ref. [29, 30]

$$B(E2, I \to I-2) = \eta^2\Delta\beta^2 n = \frac{1}{2}\eta^2\Delta\beta^2 I\,, \qquad \eta = \frac{3ZR^2}{4\pi}\,,$$

where β is the Bohr deformation parameter [29] and $\Delta\beta^2$ is its zero point amplitude

$$B(E2, I \to I-2) \propto n \propto I\,.$$

The $B(E2)$ becomes a linear function of I, i.e., $B(E2)$ increases as the spin (I) increases along the band. We calculated the increment $\Delta B(E2)$ ($\equiv B(E2)_I - B(E2)_{I-2}$) as a function of spin. We propose a fingerprint for

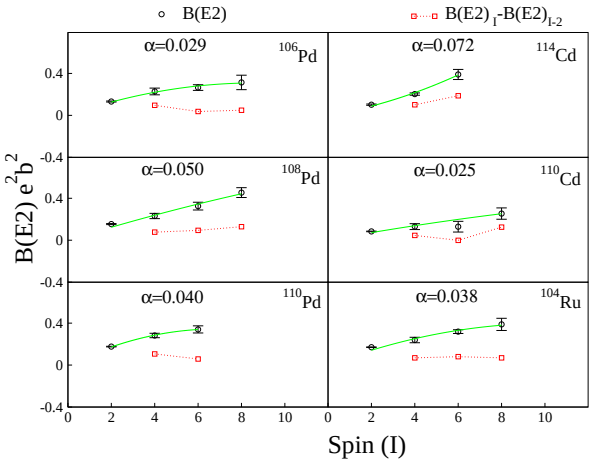

Figure 3. $B(E2)$ and $\Delta B(E2)$ values plotted against spin (I). The values of $\alpha = \triangle B(E2)/\triangle I$ is calculated for $B(E2)$ v.s. I plots. See text for details. See text for details.

tidal wave behavior: $B(E2)$ increases with spin, while $\Delta B(E2)$ decreases with spin. In contrast, both $B(E2)$ and $\Delta B(E2)$ increasing with spin would indicate a sign of vibrational band. Figure 3 illustrates $B(E2)$ and $\Delta B(E2)$ as functions of I, based on available experimental lifetime data [33]. One can notice that $B(E2)$ increases, while $\Delta B(E2)$ decreases for the isotopes ^{104}Ru, ^{106,110}Pd and ^{110}Cd. Additionally, one can notice that the slope ($\alpha = \triangle B(E2)/\triangle I$) is

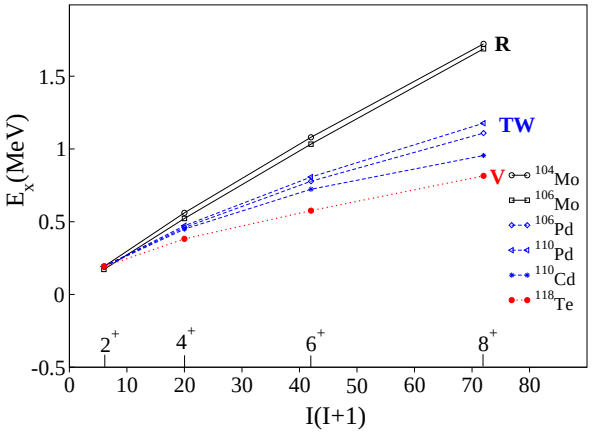

Figure 4. Energies of the yrast band members as a function of $I(I+1)$ are showing for ^{104,106}Mo (rotational-like), ^{118}Te (Vibrational) and ^{106,110}Pd, ^{110}Cd (Tidal wave). See text for details.

less than 0.05.

2.3 Excitation energies versus $I(I+1)$

Plots of spin (I) versus $\hbar\omega$ and $B(E2)$ and/or $\Delta B(E2)$ versus I indicate signatures of tidal wave behavior in ^{106,108,110}Pd and ^{110}Cd. To understand the behavior of excited state energies with respect to spin (I), the excitation energies of the yrast bands of ^{106,110}Pd and ^{110}Cd were plotted as a function of I(I+1) and compared with those of nuclei exhibiting rotational behavior ^{104,106}Mo and vibrational nature ^{118}Te in this mass region. Figure 4 presents the excitation energies as a function of I(I+1) for the yrast band members of ^{104,106}Mo (rotational-like), ^{118}Te (Vibrational) and ^{106,110}Pd, ^{110}Cd (Tidal wave).

3 Conclusions

The re-examination of nuclei within the mass range $98 \leq A \leq 118$ highlights tidal wave behavior as an intermediate phenomenon between rotational and vibrational dynamics. The proposed experimental fingerprints – increasing $B(E2)$, decreasing $\Delta B(E2)$, and large ρ values in $I(\omega)$ plots – provide a robust framework for identifying tidal wave characteristics. Notably, ^{106,110}Pd and ^{110}Cd aligns with these tidal wave fingerprints for a few yrast states, as indicated by the available experimental data. Future studies that integrate experimental observations with theoretical models such as the shell-correction version of Tilted Axis Cranking (TAC) model, are expected to further elucidate the role of tidal wave behavior in nuclear structure.

References

[1] L.K. Pattison, D.M. Cullen, J.F. Smith, A.M. Fletcher, P.M. Walker, H.M. El-Masri, Zs. Podolyák, R.J. Wood, C. Scholey, C. Wheldon, G. Mukherjee, D. Balabanski, M. Djongolov, Th. Dalsgaard, H. Thisgaard, G. Sletten, F. Kondev, D. Jenkins, G.J. Lane, I.-Y. Lee, A.O. Macchiavelli, S. Frauendorf, D. Almehed (2003) Multiphonon Vibrations at High Angular Momentum in ^{182}Os. *Phys. Rev. Lett.* **91** 182501.

[2] S. Frauendorf, Y. Gu, J. Sun (2011) Tidal waves- a non-adiabatic microscopic description of the yrast states in near-spherical nuclei. *Int. J. Mod. Phys. E* **20** 465.

[3] D.M. Cullen, R. Glover, L.K. Pattison, P.M. Walker, S. Frauendorf, D. Almehed (2005) Nuclear-tidal waves in the osmium nuclei. *J. Phys. (London) G* **31** S1709.

[4] P.H. Regan, C. Wheldon, A.D. Yamamoto, J.J. Valiente-Dobon, D. Cline, C.Y. Wu, A.O. Macchiavelli, F.R. Xu, J.F. Smith, K. Andgren, R.S. Chakrawarthy, M. Cromaz, P. Fallon, S.J. Freeman, A. Gorgen, A. Hayes, H. Hua, S.D. Langdown, I.-Y. Lee, C.J. Pearson, Zs. Podolyák, R. Teng (2005) Vibrational and rotational sequences in ^{101}Mo and ^{103,4}Ru studied via multinucleon transfer reactions. *Acta Phys. Pol. B* **36** 1313.

[5] P.H. Regan, C.W. Beausang, N.V. Zamfir, R.F. Casten, Jing-ye Zhang, A.D. Yamamoto, M.A. Caprio, G. Gürdal, A. A. Hecht, C. Hutter, R. Krücken, S.D. Langdown, D.A. Meyer, J.J. Ressler (2003) Signature for Vibrational to Rotational Evolution Along the Yrast Line. *Phys. Rev. Lett.* **90** 152502.

[6] H. Hua, C.Y. Wu, D. Cline, A.B. Hayes, R. Teng, R.M. Clark, P. Fallon, A. Goergen, A.O. Macchiavelli, K. Vetter (2004) Triaxiality and the aligned $h_{11/2}$ neutron orbitals in neutron-rich Zr and Mo isotopes. *Phys. Rev. C* **69** 014317.

[7] J. Gizon, D. Jerrestam, A. Gizon, M. Jozsa, R. Bark, B. Fogelberg, E. Ideguchi, W. Klamra, T. Lindblad, S. Mitarai, J. Nyberg, M. Piiparinen, G. Sletten (1993) Alignments and Band Termination in ^{99,100}Ru. *Z. Phys. A* **345** 335.

[8] A. Bielski, S. Brym, R. Ciuryło, J. Szudy (2000) Experimental study of speed-dependent collisional effects of He and Ne on the 687.1 nm argon line. *Eur. Phys. J. D* **8** 177.

[9] Che Xing-Lai, Zhu Sheng-Jiang, J.H. Hamilton, A.V. Ramayya, J.K. Hwang, U. Yong-Nam, Li Ming-Liang, Zheng Rang-Chen, I.Y. Lee, J.O. Rasmussen, Y.X. Luo, W.C. Ma (2004) High-Spin Structure in Neutron-Rich ^{108}Ru Nucleus. *Chin. Phys. Lett.* **21** 1904.

[10] C.Y. Wu, H. Hua, D. Cline, A.B. Hayes, R. Teng, D. Riley, R.M. Clark, P. Fallon, A. Goergen, A.O. Macchiavelli, K. Vetter (2006) Evidence for possible shape transitions in neutron-rich Ru isotopes: Spectroscopy of ^{109,110,111,112}Ru. *Phys. Rev. C* **73** 034312.

[11] Dan Jerrestam, W. Klamra, B. Fogelberg, R. Bark, A. Gizon, J. Gizon, E. Ideguchi, S. Mitarai, M. Piiparinen, G. Sletten (1996) High Spin Bands in ^{102}Pd. *Nucl. Phys. A* **603** 203.

[12] D. Sohler, I. Kuti, J. Timár, P. Joshi, J. Molnár, E.S. Paul, K. Starosta, R. Wadsworth, A. Algora, P. Bednarczyk, D. Curien, Zs. Dombrádi, G. Duchene, D.B. Fossan, J. Gál, A. Gizon, J. Gizon, D.G. Jenkins, K. Juhász , G. Kalinka, T. Koike, A. Krasznahorkay, B.M. Nyakó, P.M. Raddon, G. Rainovski, J.N. Scheurer, A.J. Simons, C. Vaman, A.R. Wilkinson, L. Zolnai (2012) High-spin structure of ^{104}Pd. *Phys. Rev. C* **85** 044303.

[13] S. Lalkovski, A. Minkova, M.-G. Porquet, A. Bauchet, I. Deloncle, A. Astier, N. Buforn, L. Donadille, O. Dorvaux, B.P.J. Gall, R. Lucas, M. Meyer, A. Prévost, N. Redon, N. Schulz, O. Stézowski (2003) Two-quasiparticle and collective excitations in transitional ^{108,110}Pd nuclei. *Eur. Phys. J. A* **18** 589.

[14] M. Houry, R. Lucas, M.-G. Porquet, Ch. Theisen, M. Girod, M. Aiche, M.M. Aleonard, A. Astier, G. Barreau, F. Becker, J.F. Chemin, I. Deloncle, T.P. Doan, J.L. Durell, K. Hauschild, W. Korten, Y. Le Coz, M.J. Leddy, S. Perries, N. Redon, A.A. Roach, J.N. Scheurer, A.G. Smith, B.J. Varley (1999)Structure of Neutron Rich Palladium Isotopes Produced in Heavy Ion Induced Fission. *Eur. Phys. J. A* **6** 43.

[15] G.A. Müller, A. Jungclaus, O. Yordanov, E. Galindo, M. Hausmann, D. Kast, K.P. Lieb, S. Brant, V. Krstić, D. Vretenar, A. Algora, F. Brandolini, G. de Angelis, M. De Poli, C. Fahlander, A. Gadea, T. Martinez, D. R. Napoli, A. Dewald, R. Peusquens, H. Tiesler, M. Górska, H. Grawe, P.G. Bizzeti (2001) High-Spin Structure and Electromagnetic Transition Strengths in ^{104}Cd. *Phys. Rev. C* **64** 014305.

[16] A.J. Simons, R. Wadsworth, D.G. Jenkins, R.M. Clark, M. Cromaz, M.A. Deleplanque, R.M. Diamond, P. Fallon, G.J. Lane, I.Y. Lee, A.O. Macchiavelli, F.S.

Stephens, C.E. Svensson, K. Vetter, D. Ward, S. Frauendorf (2003) Evidence for a New Type of Shears Mechanism in ^{106}Cd. *Phys. Rev. Lett.* **91** 162501.

[17] N.S. Kelsall, R. Wadsworth, S.J. Asztalos, B. Busse, C.J. Chiara, R.M. Clark, M.A. Deleplanque, R.M. Diamond, P. Fallon, D.B. Fossan, D.G. Jenkins, S. Juutinen, R. Krücken, G.J. Lane, I.Y. Lee, A.O. Macchiavelli, C.M. Parry, G.J. Schmid, J.M. Sears, J.F. Smith, F.S. Stephens, K. Vetter, S.G. Frauendorf (2000) Evidence for Shears Bands in ^{108}Cd. *Phys. Rev. C* **61** 011301.

[18] Santosh Roy, S. Chattopadhyay, Pradip Datta, S. Pal, S. Bhattacharya, R.K. Bhowmik, A. Goswami, H.C. Jain, R. Kumar, S. Muralithar, D. Negi, R. Palit, R.P. Singh (2011) Systematics of antimagnetic rotation in even-even Cd isotopes. *Phys. Lett. B* **694** 322.

[19] S.K. Chamoli, A.E. Stuchbery, S. Frauendorf, J. Sun, Y. Gu, R.F. Leslie, P.T. Moore, A. Wakhle, M.C. East, T. Kibédi, A.N. Wilson (2011) Measured g factors and the tidal-wave description of transitional nuclei near A = 100. *Phys. Rev. C* **83** 054318.

[20] N. Buforn, A. Astier, J. Meyer, M. Meyer, S. Perriès, N. Redon, O. Stézowski , M.G. Porquet, I. Deloncle, A. Bauchet, J. Duprat, B.J.P. Gall, C. Gautherin, E. Gueorguieva, F. Hoellinger, T. Kutsarova, R. Lucas, A. Minkova, N. Schulz, H. Sergolle, Ts. Venkova, A.N. Wilson (2000) Evidence for Deformation in $^{113-116}$Cd Isotopes. *Eur. Phys. J. A* **7** 347.

[21] G.J. Lane, D.B. Fossan, J.M. Sears, J.F. Smith, J.A. Cameron, R.M. Clark, I.M. Hibbert, V.P. Janzen, R. Krücken, I.-Y. Lee, A.O. Macchiavelli, C.M. Parry, R. Wadsworth (1998) Octupole Correlations at Low Spin in $^{108}_{52}\mathrm{Te}_{56}$. *Phys. Rev. C* **57** R1022.

[22] E.S. Paul, A.J. Boston, C.J. Chiara, M. Devlin, D.B. Fossan, S.J. Freeman, D.R. LaFosse, G.J. Lane, M.J. Leddy, I.Y. Lee, A.O. Macchiavelli, P.J. Nolan, D.G. Sarantites, J.M. Sears, A.T. Semple, J.F. Smith, K. Starosta (2007) γ-ray spectroscopy of neutron-deficient ^{110}Te. I. Low- and intermediate-spin structures. *Phys. Rev. C* **76** 034322.

[23] E.S. Paul, K. Starosta, A.O. Evans, A.J. Boston, H.J. Chantler, C.J. Chiara, M. Devlin, A.M. Fletcher, D.B. Fossan, D.R. LaFosse, G.J. Lane, I.Y. Lee, A.O. Macchiavelli, P.J. Nolan, D.G. Sarantites, J.M. Sears, A.T. Semple, J.F. Smith, C. Vaman, A V. Afanasjev, I. Ragnarsson (2007) Smooth terminating bands in ^{112}Te: Particle-hole induced collectivity. *Phys. Rev. C* **75** 014308.

[24] O. Müller, N. Warr, J. Jolie, A. Dewald, A. Fitzler, A. Linnemann, K.O. Zell, P. E. Garrett, S. W. Yates. (2005) E2 transition probabilities in ^{114}Te: A conundrum. *Phys. Rev. C* **71** 064324.

[25] P. Chowdhury, W.F. Piel, Jr., D.B. Fossan (1982) Collective Properties of $1g_{9/2}$ Proton-Hole Excitations: High-spin states in ^{116,118,120,122}Te and ^{120}Xe nuclei. *Phys. Rev. C* **25** 813.

[26] S. Juutinen, A. Savelius, P.T. Greenlees, K. Helariutta, P. Jones, R. Julin, P. Jämsen, H. Kankaanpää, M. Muikku, M. Piiparinen, S. Törmänen, M. Matsuzaki (2000) Rotational Features of Vibrator Nucleus ^{118}Te. *Phys. Rev. C* **61** 014312.

[27] A. Bohr, B.R. Mottelson (1975) "*Nuclear Structure*", Vol. II. Benjamin, New York.

[28] K.S. Krane (1988) "*Introductory Nuclear Physics*". John Wiley & Sons.

[29] J.M. Eisenberg, W. Greiner (1987) "*Nuclear Theory*", Vol. I. North Holland, Amsterdam.

[30] S. Frauendorf, M.A. Caprio, J. Sun (2012) Tidal wave in ^{102}Pd: Rotating condensate of up to seven d-bosons. WSPC Proceedings 1.

[31] N.V. Zamfir, R.F. Casten (1995) Anharmonic Vibrator Description of Yrast States of Rotational and Vibrational Nuclei. *Phys. Rev. Lett.* **75** 1280.

[32] A.O. Macchiavelli, A.D. Ayangeakaa, S. Frauendorf, U. Garg, M.A. Caprio (2014)Tidal waves in ^{102}Pd: A phenomenological analysis. *Phys. Rev. C* **90** 047304.

[33] Nuclear Data List (XUNDL), www.nndc.bnl.gov/ensdf.